Quasienergy band structure of the harmonically driven δ-function chain

D. F. Martinez and L. E. Reichl
Physics Department, The University of Texas at Austin, 1 University Station C1609, Austin, Texas 78712-0264

Germán A. Luna-Acosta
Instituto de Física, Universidad Autónoma de Puebla, Apdo. Postal J-48, Puebla, Pue, 72570, Mexico
(Received 26 July 2002; published 26 November 2002)

We study the quasienergy band structure of a potential consisting of a periodic array of harmonically oscillating δ functions. The perturbative and non-perturbative regimes are investigated using Floquet-Bloch states and the Floquet translation matrix whose eigenvalues and eigenvectors are given in terms of continued fractions. We study the structure of these eigenstates and relate it to the structure of the quasibound state of a single δ-function potential. We also study the dynamics of the bands as a function of the strength of the oscillating potential and find that the collapse of one of the quasienergy bands is related to the quenching of the transmission through a single δ-function potential.

DOI: 10.1103/PhysRevB.66.174306 PACS number(s): 72.10.Di, 73.63.−b

I. INTRODUCTION

Since the 1930s, the study of space-periodic potentials has yielded fundamental information about the properties of electrons in crystals. Tunneling and interference effects give rise to the well-known energy band structure in such materials. For real crystals, in addition to the band structure, one has to consider the interaction of the electrons with impurities or defects, the electron-electron interaction, and the electron-phonon interaction to give an accurate description of the dynamics of electrons in such materials.

The development of superlattices and the more recent advances in atom optics have brought to the forefront the study of space periodic potentials since, for the first time, it has been possible to observe fundamental quantum effects, due solely to the spatial periodicity of the potential, that had been predicted long ago. These include Landau-Zener tunneling, Wannier-Stark ladders, and Bloch oscillations, which occur in a periodic system driven by a DC electric field.[1]

The effects of time-periodic forces on spatially periodic systems have also been studied and interesting phenomena have been predicted (and some observed experimentally) such as dynamical localization (mini-band collapse),[2,3] photon-assisted tunneling,[4] quantum Hamiltonian ratchets,[5,6] chaos-assisted tunneling,[7–11] dynamic Anderson-localization[12] and quantization of particle transport.[13]

Because of the myriad of phenomena that have been associated with space-time periodic potentials, it is interesting to study one of the simplest potentials which has both periodicities: a spatially periodic chain of δ-function potentials whose strength oscillates periodically in time. The mathematical simplicity of this potential permits an analytic computation of its eigenstates and eigenvalues with the use of continued fractions. This simplicity also allows for a clear understanding of the basic dynamical properties of a quantum particle under a space-time periodic potential. This system is special because its classical analog is quasi-integrable,[14] whereas most other systems of this type are non-integrable.

In Sec. II we derive the Floquet-Bloch (FB) Hamiltonian for the oscillating delta chain and use it to investigate the quasienergy (QE) band structure in the perturbative regime. In Sec. III we construct the Floquet translation matrix (TM). In Sec. IV, we solve for the eigenvalues and eigenvectors of the TM matrix using continued fractions. In Sec. V, we study the structure of the eigenvectors in the negative energy channels and relate it to some scattering properties of the single δ-function potential which are derived in Appendices A and B. In Sec. VI, we study how the QE band structure changes as a function of the strength of the oscillating potential. And finally in Sec. VII, we make some concluding remarks.

II. FLOQUET-BLOCH APPROACH

The Hamiltonian we will study in this paper is of the form

$$H=\frac{p^2}{2\mu}+[\tilde{V}_0+\tilde{V}_1\cos(\omega t)]\sum_{m=-\infty}^{\infty}\delta(x-mL). \qquad (1)$$

Here, p and x are the momentum and position operators, μ is the effective mass of the particle, $\tilde{V}_0$ is the strength of the static part of the potential, $\tilde{V}_1$ is the strength of the oscillating part of the potential, ω is the frequency of the oscillation, t is the time, and L is the distance between neighboring delta functions.

Since a wave function that satisfies Schrödinger's equation $i\hbar(\partial\Psi/\partial t)=H\Psi$ with Hamiltonian (1) must be periodic in time and space (Floquet-Bloch theorem), the solutions are of the form

$$\Psi_{\epsilon,\kappa}(x,t)=e^{-i\epsilon t/\hbar}e^{i\kappa x}\sum_{n=-\infty}^{\infty}\sum_{m=-\infty}^{\infty}\psi_{n,m}e^{2\pi mi(x/L)}e^{-in\omega t}, \qquad (2)$$

where $\hbar$ is Planck's constant, $\psi_{n,m}$ is a probability amplitude, ϵ is the quasienergy (with allowed values $0\leqslant\epsilon\leqslant\hbar\omega$), and κ is the Bloch momentum (for which the first Brillouin zone is taken to be $-\pi/L\leqslant\kappa\leqslant\pi/L$). If we substitute the state $\Psi_{\epsilon,\kappa}(x,t)$ into the Schrodinger equation and use the fact that $(1/L)\int_{-L/2}^{L/2}dx\exp[2\pi i/L(m-m')x]$

$=\delta_{m,m'}$,$(1/T)\int_o^T dt\,\exp[i\omega(n-n')t]=\delta_{n,n'}$, we obtain an eigenvalue equation for the amplitude $\psi_{n,m}$,

$$\sum_{n'=-\infty}^{\infty}\sum_{m'=-\infty}^{\infty}\tilde{H}^{\mathrm{FB}}_{n,n',m,m'}\psi_{n',m'}=\epsilon\ \ \psi_{n,m}, \tag{3}$$

where $\tilde{H}^{\mathrm{FB}}$ is the FB Hamiltonian

$$\tilde{H}^{\mathrm{FB}}_{n,n',m,m'}=\left[\frac{\hbar^2}{2\mu}\left(\kappa+\frac{2\pi}{L}m\right)^2-n\hbar\omega\right]\delta_{n,n'}\delta_{m,m'}+\frac{\tilde{V}_0}{L}\delta_{n,n'}+\frac{\tilde{V}_1}{2L}(\delta_{n-1,n'}+\delta_{n+1,n'}). \tag{4}$$

Diagonalization of this matrix yields the quasienergies and eigenvectors as a function of the Bloch-momentum κ:

For computational purposes, it is convenient to define the following dimensionless quantities,

$$\varepsilon\equiv\epsilon/\hbar\omega,\quad l\equiv L\sqrt{\frac{2\mu\omega}{\hbar}},\quad k\equiv\kappa\sqrt{\frac{\hbar}{2\mu\omega}},$$

$$x'\equiv x\sqrt{\frac{2\mu\omega}{\hbar}},\quad \tau=\omega t, \tag{5}$$

$$V_1\equiv\frac{\mu\tilde{V}_1}{2\hbar^2\sqrt{2\mu\omega/\hbar}},\quad V_0\equiv\frac{\mu\tilde{V}_0}{\hbar^2\sqrt{2\mu\omega/\hbar}},\quad H^{\mathrm{FB}}\equiv\tilde{H}^{\mathrm{FB}}/\hbar\omega.$$

In terms of these dimensionless variables, the FB Hamiltonian takes the form

$$H^{\mathrm{FB}}_{n,n',m,m'}=\left(\frac{1}{l^2}(kl+2\pi m)^2-n\right)\delta_{n,n'}\delta_{m,m'}+2\frac{V_0}{l}\delta_{n,n'}+2\frac{V_1}{l}(\delta_{n-1,n'}+\delta_{n+1,n'}). \tag{6}$$

For zero static potential, $V_0=0$, and small V_1, the quasienergy bands can be labeled away from the avoided crossings, by the integer pair (n,m) as is shown in Fig. 1 for the parameters $V_1=0.03,l=5$. The FB eigenvector corresponding to the point $\varepsilon_{(n,m)}(kl)$ on band (n,m), is a plane wave with (dimensionless) energy $E=(n+\varepsilon)$ and (dimensionless) momentum $K=k+(2\pi/l)m$. The curve in Fig. 1 for the pair (n,m) is obtained by drawing a parabola centered at the point $(n,2\pi m)$ in the infinite plane (E,K). The segment of the parabola that crosses the region $0\leqslant E\leqslant 1$, $-\pi/l<K\leqslant\pi/l$, gives rise to the quasienergy band labeled (n,m).

It is also useful to plot the average energy of the FB eigenstates, $\Psi_{\epsilon,\kappa}(x,t)$, which we define as

$$\langle E\rangle\equiv\sum_n(\varepsilon+n)\sum_m|\psi_{n,m}|^2. \tag{7}$$

This is shown in Fig. 2 for the same parameters chosen for Fig. 1. Let us focus on three features, marked A,B,C, in Figs. 1 and 2. We begin by studying B, an avoided crossing between bands $(1,-1)$ and $(2,1)$. From first-order degenerate perturbation theory we obtain the reduced 2×2 Hamiltonian near the point $kl\sim1$:

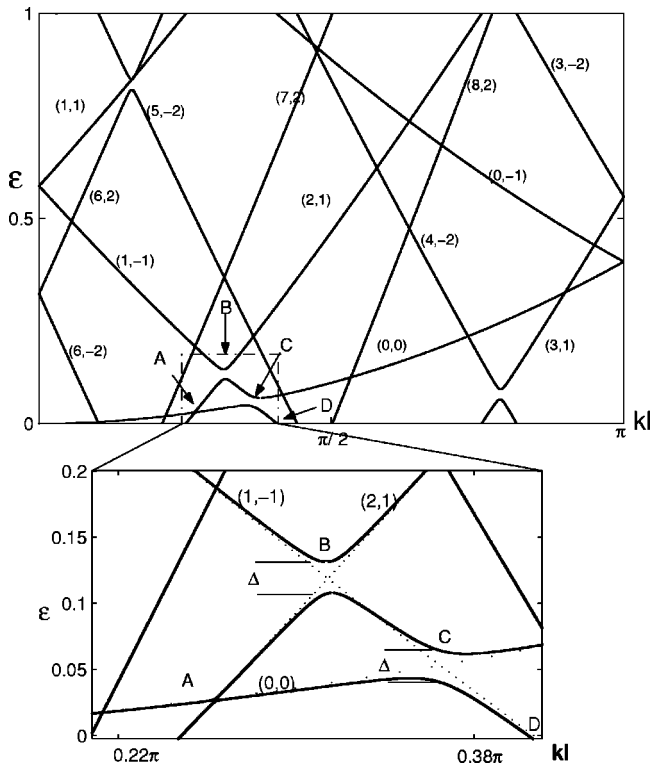

FIG. 1. Quasienergy curves for $V_0=0,V_1=0.03,l=5$. Curves have been labeled using (n,m) pairs, where the energy of the corresponding unperturbed state is $E=(n+\varepsilon)\hbar\omega$, and its wave vector is $K=k+2\pi m/l$. Features *A*, *B*, *C*, and *D* are indicated. The inset shows a magnification of the dashed box.

$$H^{\mathrm{FB}}=\begin{bmatrix}\varepsilon^0_{1,-1}(kl) & 2\dfrac{V_1}{l}\\ 2\dfrac{V_1}{l} & \varepsilon^0_{2,1}(kl)\end{bmatrix}, \tag{8}$$

where the unperturbed quasienergies are $\varepsilon^0_{1,-1}(kl)=\frac{1}{25}(kl-2\pi)^2-1,\varepsilon^0_{2,1}(kl)=\frac{1}{25}(kl+2\pi)^2-2$. The eigenvalues of this Hamiltonian matrix give the quasienergy bands in the neighborhood of the crossing,

$$\varepsilon^{\pm}(kl)=\tfrac{1}{2}[\varepsilon^0_{1,-1}(kl)+\varepsilon^0_{2,1}(kl)]\pm\tfrac{1}{2}\sqrt{[\varepsilon^0_{1,-1}(kl)-\varepsilon^0_{2,1}(kl)]^2+16\left(\frac{V_1}{l}\right)^2}. \tag{9}$$

At the middle of the avoided crossing, where $\varepsilon^0_{1,-1}=\varepsilon^0_{2,1}$, the distance between the bands, Δ, is

$$\Delta=4\frac{V_1}{l}. \tag{10}$$

Note that the width of the avoided crossing does not depend on the energy or momentum of the bands involved, which is

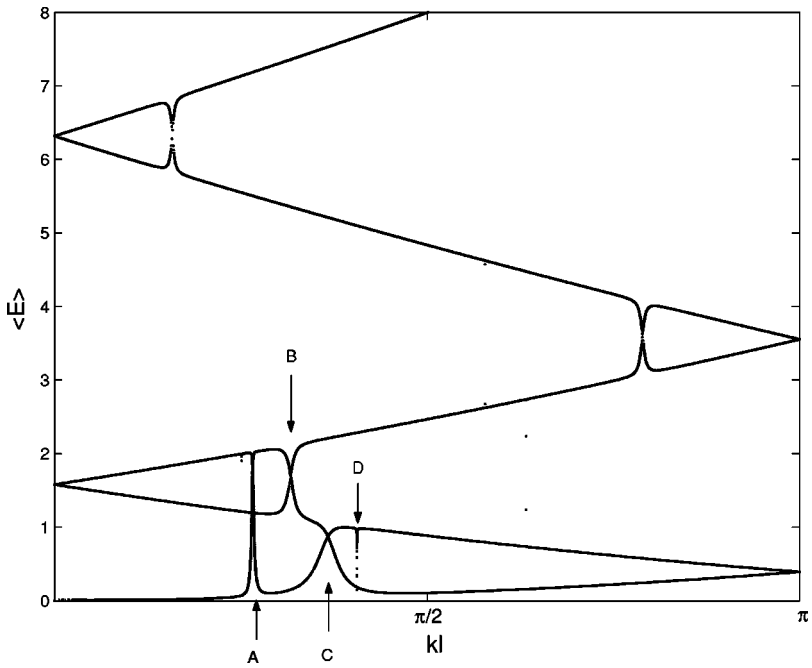

FIG. 2. Average energy, $\langle E \rangle$, vs Bloch momentum, k, for $V_0=0, V_1=0.03, l=5$. Features *A*, *B*, *C*, and *D* (discussed in the text) are indicated.

a peculiar feature of the delta-function chain. Therefore, for the delta-function chain, all first-order avoided crossings have the same width, Δ.

Feature C is an example of a first-order avoided crossing between bands (0,0) and (1,−1). Note that the first-order avoided crossings in the quasienergy plot reveal themselves as crossings in the average energy plot. This happens because at an avoided crossing the two states exchange identities, and the average energy includes the contribution from both states.

Feature A, in Fig. 2, is a second-order avoided crossing, involving a two phonon process between the unperturbed states (2,1) and (0,0). This is evident in Fig. 2, where the crossing occurs between a band with average energy near $2\hbar\omega$ and a band near $0\ \hbar\omega$.

Feature D in Fig. 2 cannot be explained using degenerate perturbation theory. It is not the result of an avoided crossing between unperturbed states. This feature occurs when the unperturbed quasienergy band (1,−1) (in Fig. 1) crosses the lower edge of the quasienergy Brillouin zone ($\varepsilon=0$). This sudden drop in the average energy of the eigenstate will be discussed in Sec. IV.

III. TRANSLATION MATRIX

Let us now construct the Floquet translation matrix for the δ-function chain. This will be done in two steps. First, we calculate the transfer matrix connecting the Floquet coefficients of the wave function [Eq. (2)] on the left and on the right of a δ function. Then we calculate the translation matrix which connects the Floquet components of the wave function on the left side of a delta function with the components on the left side of the nearest neighbor delta function. The eigenvectors of this translation matrix will have either pure real (norm of eigenvalue equal to one) or complex (norm different from one) Bloch momentum. The cases with real Bloch momentum correspond to the physical states, while the eigenfunctions with complex Bloch momentum are not physical since they diverge in one direction along the x axis.

A. Time periodicity

Let us write the FB state, $\Psi_{\epsilon,\kappa}(x,t)$, in terms of dimensionless variables, and in the form

$$\Psi_{\varepsilon}(x',\tau)=\sum_{n=-\infty}^{\infty}\psi_n(x')e^{-i(\varepsilon+n)\tau}, \tag{11}$$

where $\psi_n(x')$ contains all the spatial dependance of the wave function. Since the potential is zero everywhere except at $x'=ml$, we assume $\psi_n(x')$ in regions I and II (on the left and right of the δ function at $x'=0$, respectively) to be of the form

$$\psi_n^{\mathrm{I}}(x')=\frac{1}{\sqrt{k_n}}(a_n e^{ik_n x'}+d_n e^{-ik_n x'}) \quad \text{for } -l<x<0,$$
$$\psi_n^{\mathrm{II}}(x')=\frac{1}{\sqrt{k_n}}(c_n e^{ik_n x'}+b_n e^{-ik_n x'}) \quad \text{for } 0<x<l. \tag{12}$$

For finite chains, the factor $1/\sqrt{k_n}$ is included to ensure unitarity of the S matrix;[15] we also use that convention here. The dimensionless wave vectors, k_n, are given by

$$k_n\equiv\sqrt{\varepsilon+n}. \tag{13}$$

Note that for $n<0$ the wave vector is imaginary and gives rise to exponentially decaying and growing modes. These will be discussed later in Sec. V.

Continuity of $\Psi_{\varepsilon}(x',\tau)$ at $x'=0$ gives

$$a_n+d_n=c_n+b_n. \tag{14}$$

Because of the delta function in the Hamiltonian, the spatial derivative of $\Psi_\varepsilon(x',\tau)$ at $x'=0$ is discontinuous and satisfies

$$\left.\frac{d\Psi_\varepsilon}{dx'}\right|_{x'=0^+} - \left.\frac{d\Psi_\varepsilon}{dx'}\right|_{x'=0^-} = [V_0 + V_1\cos(\tau)]\Psi_\varepsilon(0,\tau). \tag{15}$$

This leads to the condition

$$c_n + d_n - b_n - a_n = -2i[s_n(a_n+d_n) + h_{n-1}(a_{n-1}+d_{n-1}) + h_n(a_{n+1}+d_{n+1})], \tag{16}$$

where

$$h_n = \frac{V_1}{(\varepsilon+n)^{1/4}(\varepsilon+n+1)^{1/4}}, \quad s_n = \frac{V_0}{\sqrt{\varepsilon+n}}. \tag{17}$$

Using Eqs. (14) and (16) we solve for c_n and b_n in terms of a_n and d_n to obtain

$$c_n = a_n - is_n a_n - ih_{n-1}a_{n-1} - ih_n a_{n+1} - is_n d_n - ih_{n-1}d_{n-1} - ih_n d_{n+1} \tag{18}$$

and

$$b_n = d_n + is_n a_n + ih_{n-1}a_{n-1} + ih_n a_{n+1} + is_n d_n + ih_{n-1}d_{n-1} + ih_n d_{n+1}. \tag{19}$$

It is useful to define the column vectors **A**, **B**, **C**, and **D** with components a_n, b_n, c_n, and d_n, respectively. Then Eqs. (18) and (19) can be written in matrix form as

$$\mathbf{C} = (\mathbf{1}-\mathbf{X})\cdot\mathbf{A} - \mathbf{X}\cdot\mathbf{D}, \tag{20}$$

$$\mathbf{B} = \mathbf{X}\cdot\mathbf{A} + (\mathbf{1}+\mathbf{X})\cdot\mathbf{D}, \tag{21}$$

where the matrix **X** has components

$$[X]_{n,n'} = \delta_{n',n-1}ih_{n'} + \delta_{n',n+1}ih_{n'-1} + \delta_{n',n}is_n. \tag{22}$$

This system of equations can also be written as

$$\begin{pmatrix}\mathbf{C}\\ \mathbf{B}\end{pmatrix} = \mathbf{M}\cdot\begin{pmatrix}\mathbf{A}\\ \mathbf{D}\end{pmatrix} \tag{23}$$

with

$$\mathbf{M} = \begin{bmatrix}\mathbf{1}-\mathbf{X} & -\mathbf{X}\\ \mathbf{X} & \mathbf{1}+\mathbf{X}\end{bmatrix}. \tag{24}$$

The matrix M relates components of the eigenstates on opposite sides of a single δ function in the infinite chain.

B. Spatial periodicity

Because of the spatial periodicity of the Hamiltonian Eq. (1), Floquet-Bloch states have the property

$$\mathcal{T}^l\Psi_{\varepsilon,k}(x') = \Psi_{\varepsilon,k}(x'+l) = \lambda\Psi_{\varepsilon,k}(x'), \tag{25}$$

where $\mathcal{T}^l$ is the spatial translation operator and λ is its eigenvalue, which satisfies $\lambda = e^{ikl}$ for k real when $\Psi_{\varepsilon,k}(x')$ is a Bloch function. Imposing this condition on the wave function and its derivative at the point $x' = -l/2$, we obtain

$$\begin{aligned}\lambda(a_n e^{-ik_n l/2} + d_n e^{ik_n l/2}) &= c_n e^{ik_n l2} + b_n e^{-ik_n l/2},\\ \lambda(a_n e^{-ik_n l/2} - d_n e^{ik_n l/2}) &= c_n e^{ik_n l/2} - b_n e^{-ik_n l/2}.\end{aligned} \tag{26}$$

We can write this set of equations as

$$\lambda\begin{bmatrix}\mathbf{T}_{-l/2} & \mathbf{T}_{l/2}\\ \mathbf{T}_{-l/2} & -\mathbf{T}_{l/2}\end{bmatrix}\begin{pmatrix}\mathbf{A}\\ \mathbf{D}\end{pmatrix} = \begin{bmatrix}\mathbf{T}_{l/2} & \mathbf{T}_{-l/2}\\ \mathbf{T}_{l/2} & -\mathbf{T}_{-l/2}\end{bmatrix}\begin{pmatrix}\mathbf{C}\\ \mathbf{B}\end{pmatrix}, \tag{27}$$

where the matrix $T_{\pm l/2}$ is diagonal and has matrix elements $e^{\pm ik_n l/2}$. We can now write

$$\begin{aligned}\lambda\begin{pmatrix}\mathbf{A}\\ \mathbf{D}\end{pmatrix} &= \begin{bmatrix}\mathbf{T}_{-l/2} & \mathbf{T}_{l/2}\\ \mathbf{T}_{-l/2} & -\mathbf{T}_{l/2}\end{bmatrix}^{-1}\begin{bmatrix}\mathbf{T}_{l/2} & \mathbf{T}_{-l/2}\\ \mathbf{T}_{l/2} & -\mathbf{T}_{-l/2}\end{bmatrix}\begin{pmatrix}\mathbf{C}\\ \mathbf{B}\end{pmatrix}\\ &= \frac{1}{2}\begin{bmatrix}\mathbf{T}_{l/2} & \mathbf{T}_{l/2}\\ \mathbf{T}_{-l/2} & -\mathbf{T}_{-l/2}\end{bmatrix}\begin{bmatrix}\mathbf{T}_{l/2} & \mathbf{T}_{-l/2}\\ \mathbf{T}_{l/2} & -\mathbf{T}_{-l/2}\end{bmatrix}\begin{pmatrix}\mathbf{C}\\ \mathbf{B}\end{pmatrix}\\ &= \begin{bmatrix}\mathbf{T}_l & \mathbf{0}\\ \mathbf{0} & \mathbf{T}_{-l}\end{bmatrix}\begin{pmatrix}\mathbf{C}\\ \mathbf{B}\end{pmatrix}.\end{aligned} \tag{28}$$

If combine Eqs. (23), (24), and (28), we obtain

$$\mathbf{TM}\begin{pmatrix}\mathbf{A}\\ \mathbf{D}\end{pmatrix} = \lambda\begin{pmatrix}\mathbf{A}\\ \mathbf{D}\end{pmatrix}, \tag{29}$$

where

$$\mathbf{TM} = \begin{bmatrix}\mathbf{T}_l(\mathbf{1}-\mathbf{X}) & -\mathbf{T}_l\mathbf{X}\\ \mathbf{T}_{-l}\mathbf{X} & \mathbf{T}_{-l}(\mathbf{1}+\mathbf{X})\end{bmatrix} \tag{30}$$

is the Floquet translation matrix. After diagonalizing the TM matrix, one selects the eigenvectors corresponding to eigenvalues $|\lambda| = 1$. These are the Floquet-Bloch states of the system.

C. Static potential case ($V_0 \neq 0, V_1 = 0$)

For a purely static potential, the TM matrix is a 2×2 matrix with two distinct eigenvalues and corresponding eigenvectors. It can be shown that

$$\mathrm{TM} = \begin{bmatrix} e^{ikl}\left(1+\frac{Vo}{2ik}\right) & e^{ikl}\left(\frac{Vo}{2ik}\right)\\ e^{-ikl}\left(-\frac{Vo}{2ik}\right) & e^{-ikl}\left(1-\frac{Vo}{2ik}\right)\end{bmatrix}, \tag{31}$$

where $k = \sqrt{2E}$.

A graph of the absolute value of the two eigenvalues of TM, as a function of energy, for the static delta chain is shown in Fig. 3(a). The prohibited energy regions are the regions occupied by the ''bubbles.'' These occur at energies for which the absolute value of the eigenvalues of TM is not one. The well-known band structure for this potential is obtained by plotting energy versus Bloch momentum as shown in Fig. 3(b). For the parameters chosen in Fig. 3, the delta-

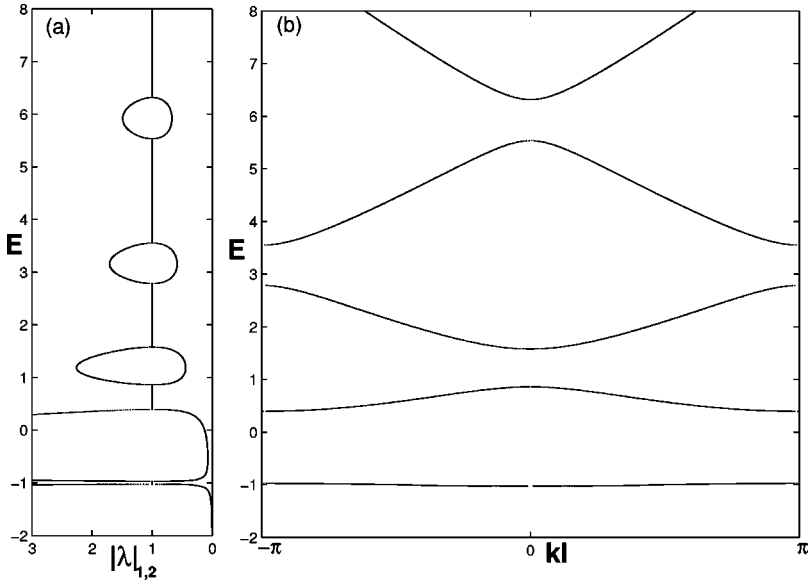

FIG. 3. (a) Energy, E, plotted as a function of the absolute value of eigenvalues $\lambda_{1,2}$ of the TM matrix (measured in units of the bound-state energy of one δ-function potential, $E_{\text{bound}} = -\mu V_o^2/2\hbar^2 = -1$). (b) Energy vs Bloch momentum, k, for a static chain. Parameters used are $V_0 = -\sqrt{2}$, $V_1 = 0$, $l = 5$, $\mu = 1$, and $\hbar = 1$.

function potential has a bound state at $E = -1$. That is precisely the location of the negative energy band, which occupies the region $-1.025 < E < -0.975$. The width of this band is known to decrease rapidly with the distance between wells.[22] For $l = 5$ it is already of the order of 10^{-3}.

It is now interesting to use the Floquet TM matrix derived in Secs. III A and III B for the case when $V_0 \neq 0, V_1 = 0$ as a way to test the Floquet formalism and to gain insight into the effect of a time periodic perturbation in the band structure of the static potential. Using the Floquet TM matrix of Eq. (30) and the same parameters is in Fig. 3, we obtain in Fig. 4(a), a plot of the eigenvalues of the TM matrix as a function of the quasienergy. In Fig. 4(b), we obtain a plot of the quasienergy versus Bloch momentum. The relation between Fig. 4 and Fig. 3 is simple. The energy axes in Figs. 3(a) and 3(b) have been divided into intervals of width $\hbar\omega$ and the intervals have been mapped into the region $0 \leqslant \epsilon \leqslant \hbar\omega$ in Figs. 4(a) and 4(b), respectively. The way to recover the results in Fig. 3 starting with Fig. 4 is to ''unfold'' the quasienergy axis by calculating the ''average'' energy, as defined in Eq. (7), for each eigenvector in the QE bands. This shows us that when the oscillating part of the potential is small compared to the static part, the quantity that approximately preserves the band structure of the static potential is $\langle E \rangle$. The effect of a small oscillating potential is only important when the distance between two unperturbed energy bands is a multiple of $\hbar\omega$ (in the neighborhood of a quasienergy avoided crossing); this is where the deviations of $\langle E \rangle$ from the band structure of the static potential occur, as was shown in Sec. II, Figs. 1 and 2. Thus, the average energy is a useful quantity since it smoothly becomes the energy as the oscillating potential is turned off.

IV. EIGENVECTORS OF THE FLOQUET TRANSLATION MATRIX

The solution to the eigenvalue equation [Eq. (29)] can be obtained in terms of continued fractions. The procedure we

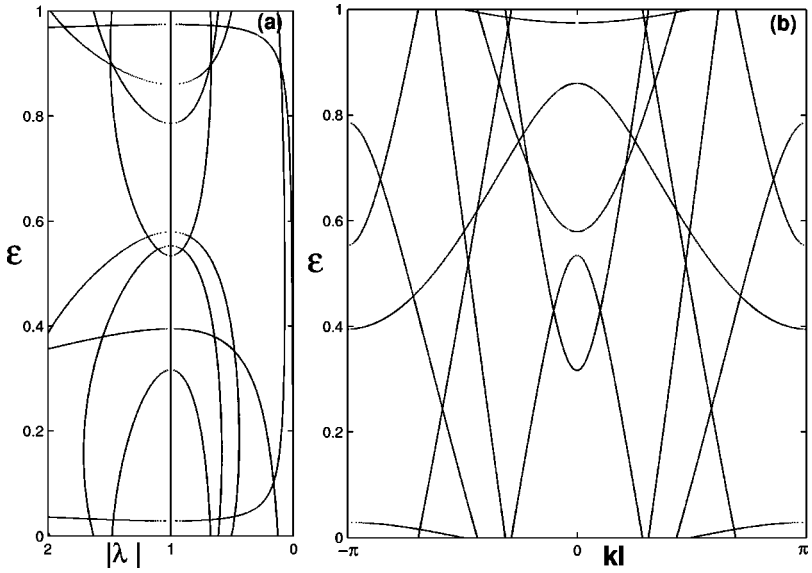

FIG. 4. (a) Quasienergy, ε, vs the absolute value of the eigenvalues λ of the Floquet TM matrix. (b) Quasienergy, ε, vs the Block momentum, k. Parameters used are $V_0 = -\sqrt{2}$, $V_1 = 0$, and $l = 5$. Only 8 positive energy channels included.

follow is similar to the one used in the study of the scattering properties of a single oscillating δ-function potential.[15]

Equation (29) can be written in the form

$$(\mathbf{1}-\mathbf{X})\cdot\mathbf{A}-\mathbf{X}\cdot\mathbf{D}=\lambda\mathbf{T}_{-l}\cdot\mathbf{A},$$

$$(\mathbf{1}+\mathbf{X})\cdot\mathbf{D}+\mathbf{X}\cdot\mathbf{A}=\lambda\mathbf{T}_{l}\cdot\mathbf{D}. \tag{32}$$

Adding these two equations, we obtain a relationship between the components of **A** and **D**,

$$D_n=\eta_n A_n,$$

with

$$\eta_n=-\frac{1-e^{ikl}e^{-ik_nl}}{1-e^{ikl}e^{ik_nl}}, \tag{33}$$

where the dimensionless quantities k_n, k, and l [defined in Eqs. (5) and (13)] have been used. The relation between A and D is purely kinematic; it does not depend on the potential. If we combine Eqs. (32) and (33), we obtain

$$(\mathbf{1}-\lambda\mathbf{T}_{-l})\cdot\mathbf{A}=\mathbf{X}\cdot\mathbf{P}\cdot\mathbf{A}, \tag{34}$$

where **P** is a diagonal matrix with matrix elements

$$P_n\equiv[\mathbf{P}]_{n,n}=\frac{e^{-ik_nl}-e^{ik_nl}}{1-e^{ikl}e^{ik_nl}}e^{ikl}. \tag{35}$$

We now define

$$Q_n=[\mathbf{1}-\lambda\mathbf{T}_{-l}]_{n,n}=1-e^{-ik_nl}e^{ikl}. \tag{36}$$

Using this, and Eq. (22) we obtain from Eq. (34),

$$R_n a_n-ih_{n-1}P_{n-1}a_{n-1}=ih_nP_{n+1}a_{n+1}, \tag{37}$$

where

$$R_n=Q_n-is_nP_n. \tag{38}$$

Using the method of continued fractions we now obtain from Eq. (37) an expression for the ratio a_n/a_{n+1}. Let us define

$$f_n=\frac{a_n}{a_{n+1}}. \tag{39}$$

If we substitute Eq. (39) into Eq. (37), we obtain

$$R_n-ih_{n-1}P_{n-1}f_{n-1}=\frac{ih_nP_{n+1}}{f_n}. \tag{40}$$

Solving Eq. (40) for f_n in terms of f_{n-1} gives

$$f_n=\frac{ih_nP_{n+1}}{R_n-ih_{n-1}P_{n-1}f_{n-1}}, \tag{41}$$

and solving Eq. (40) for f_{n-1} in terms of f_n gives

$$f_{n-1}=\frac{1}{ih_{n-1}P_{n-1}}\left(R_n-\frac{ih_nP_{n+1}}{f_n}\right). \tag{42}$$

Thus, from Eqs. (41) and (42), we can obtain two different expressions for the quantity f_n. If we iterate Eq. (41) we obtain

$$f_n^{\downarrow}=\cfrac{ih_nP_{n+1}}{R_n+\cfrac{h_{n-1}^2P_{n-1}P_n}{R_{n-1}+\cfrac{h_{n-2}^2P_{n-2}P_{n-1}}{R_{n-2}+\cfrac{h_{n-3}^2P_{n-3}P_{n-2}}{\vdots}}}}, \tag{43}$$

where the downward arrow indicates that the indices of all quantities (except P_{n+1}) run over integers equal to or smaller than n. If we iterate Eq. (42) we obtain

$$f_n^{\uparrow}=\frac{1}{ih_nP_n}\left(R_{n+1}+\cfrac{h_{n+1}^2P_{n+1}P_{n+2}}{R_{n+2}+\cfrac{h_{n+2}^2P_{n+2}P_{n+3}}{R_{n+3}+\cfrac{h_{n+3}^2P_{n+3}P_{n+4}}{\vdots}}}\right), \tag{44}$$

where the upward arrow indicates that the indices of all quantities run over integers equal or greater than n. It is important to note that these two functions have very different dependence on n. When $|n|\to\infty$, $f_n^{\uparrow}\to\infty$. This implies that for $|n|$ large, $a_n\gg a_{n+1}$ (the components of the eigenvector decay for n positive and grow for n negative). On the other hand, when $|n|\to\infty$, $f_n^{\downarrow}\to 0$. This implies that for $|n|$ large $a_n\ll a_{n+1}$ (the components of the eigenvector grow for n positive and decay for n negative). This means that to obtain eigenvectors that have support in a finite number of channels one has to use $f_n^{\uparrow}$ for $n\gg 1$ and $f_n^{\downarrow}$ for $n\ll -1$.

We can now derive a general prescription to generate the components of an eigenvector starting from an arbitrary $a_n=1$. By applying repeatedly the definition of $f_n=a_n/a_{n+1}$, we obtain

$$a_{m+n}=\frac{a_m}{f_{m+n-1}^{\uparrow}f_{m+n-2}^{\uparrow}\cdots f_m^{\uparrow}}, \tag{45a}$$

$$a_{m-n}=f_{m-1}^{\downarrow}f_{m-2}^{\downarrow}\cdots f_{m-n}^{\downarrow}a_m \tag{45b}$$

for any $n>0$. One can avoid having to use both equations to generate the components of an eigenvector by using Eq. (45a) and starting with an m negative enough so that all eigenvectors have support on channels higher than m. This can be done since for any eigenvector, and for n negative and large, $a_n\ll a_{n+1}$. Then, the contribution of large negative components to any eigenvector will be negligible.

Let us now define the function,

$$\Pi_n(\varepsilon,k)=\Pi_{i=-m}^{n}\frac{1}{f_i^{\uparrow}(\varepsilon,k)}, \tag{46}$$

where m is chosen so all eigenvectors have support on channels higher than m. Using this function we can construct the positive momentum components of any eigenvector Ψ^T

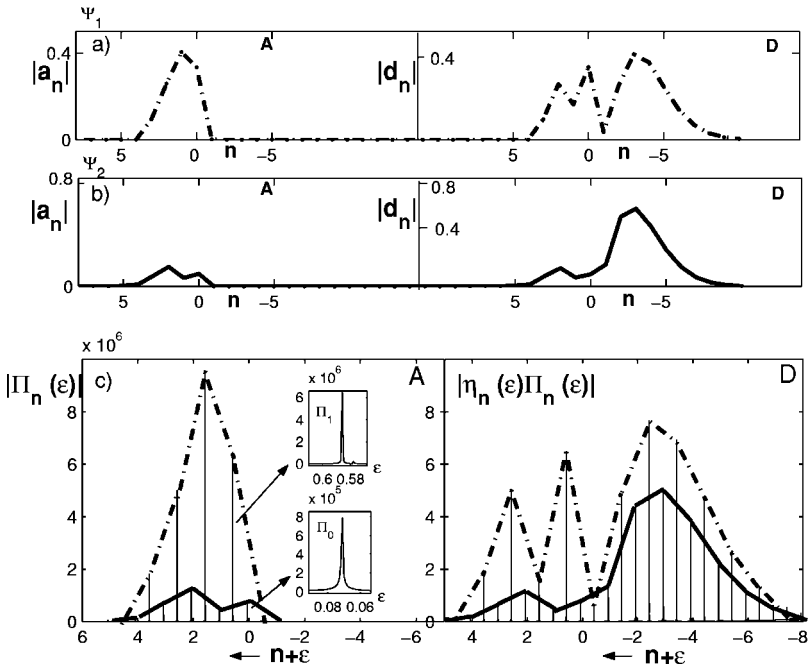

FIG. 5. Plots of components of **A** and **D** for two FB eigenvectors with $(\varepsilon=0.586,k=0.01)$ and $(\varepsilon=0.07,k=0.01)$ for $V_0=0,V_1=1.0,l=5$. (a) Eigenvector of the TM matrix with $(\varepsilon=0.586,k=0.01)$. (b) Eigenvector of the TM matrix with $(\varepsilon=0.07,k=0.01)$. (c) Plots of **A** and **D** obtained from Eqs. (47) and (33). These plots are indicative of the pole structure of Π_n. The dashed line corresponds to $(\varepsilon=0.586,k=0.01)$ and the solid line to $(\varepsilon=0.07,k=0.01)$.

$=(\mathbf{A^T},\mathbf{D^T})$, where T denotes transpose, starting with an arbitrarily fixed $a_{-m}=1$ (before the vector is normalized). We can write

$$\mathbf{A}^T=[\ \ldots,1,\Pi_{-m}(\varepsilon,k),\Pi_{-m+1}(\varepsilon,k),\ \ldots,\Pi_n(\varepsilon,k),\ \ldots\ ]. \tag{47}$$

The negative momentum components, **D**, are obtained from Eq. (33).

For any point (ε,k) chosen, there is a band that passes arbitrarily close to that point (the bands fill the first Brillouin zone densely). At this point, several components Π_n have a pole. Each diverging Π_n gives a nonzero component of the eigenvector corresponding to this point. After obtaining the D components and normalizing we end up with the full eigenvector which can be compared to the eigenvectors obtained from direct numerical diagonalization of the matrix TM at the same point.

We have now developed three different methods to obtain Floquet-Bloch states for our system. (1) We can find the eigenvectors of the F.B. Hamiltonian, Eq. (6). (2) We can find the poles of Eq. (47). (3) We can find by numerical diagonalization the eigenvectors of the TM matrix in Eq. (30). In the first two approaches, one specifies both the quasienergy and the Bloch momentum, and then one proceeds to find the corresponding eigenvector. In the third approach, Eq. (30), only the quasienergy is required, the Bloch momentum is a result of the calculation of the eigenvalues of the TM matrix.

In Figs. 5(a) and 5(b), we show a plot of two eigenfunctions obtained by constructing the translation matrix, TM, for parameters $V_1=1.0,V_0=0$, and then numerically finding its eigenvalues and eigenvectors. Eigenvector Ψ_1 has quantum numbers, $(\varepsilon=0.586,k=0.01)$, and eigenvector Ψ_2 has quantum numbers, $(\varepsilon=0.07,k=0.01)$. In Fig. 5(c) we show a graph of the positive momentum components, **A**, and negative momentum components, **D**, of these eigenvectors as a function of ε for $k=0.01$, calculated using Eqs. (47) and (33). The components are arranged in decreasing order of energy (from left to right). There are very narrow peaks for all components shown, at quasienergies 0.586 and 0.07 as can be seen in the insets. The profile of an eigenstate, as obtained by connecting its corresponding peaks, is in very good agreement with the results obtained by diagonalizing the TM matrix.

By plotting the component $\Pi_8(\varepsilon,k)$ in the interval $0\leqslant\varepsilon\leqslant1,0\leqslant kl\leqslant\pi$, one can see the band structure of this potential. We include bands whose eigenvectors have components in channels $n'\leqslant8$. Figure 6(a) shows a contour plot of values of $\Pi_8(\varepsilon,k)$. Figure 6(b) shows the QE bands obtained by diagonalizing TM.

As mentioned earlier, feature D in Fig. 2 cannot be explained using degenerate perturbation theory because it is not the result of an avoided crossing. To examine this feature let us consider the functions $f_0^{\downarrow}$ and $f_{-1}^{\downarrow}$, [see Eq. (43)]. When $\varepsilon\to0$, $h_0\sim1/\sqrt{k_0}\to\infty$, $h_{-1}\sim1/\sqrt{k_0}\to\infty$, and $P_0\sim k_0\to0$. Therefore $f_0^{\downarrow}\to\infty$ when $\varepsilon\to0$, which implies $a_0/a_1\to\infty$. One can also show that $f_{-1}^{\downarrow}\to0$ as $\varepsilon\to0$, which implies $a_0/a_1\to\infty$. This means that a_0 is the only non-zero component of an eigenvector corresponding to a quasienergy band at the point $\varepsilon=0$. Therefore, the average energy of the eigenvector goes to zero at this point. This explains the plunge observed in Fig. 2 at point D. In principle there should be a feature like D for any band that crosses the line $\varepsilon=0$. However, the width of the ''plunge'' in the average energy band depends on the size of the component a_1 of the eigenvector as one approaches the bottom of the energy Brillouin zone. The higher the average energy of the band where the plunge occurs, the narrower it is, because the a_1 component of the eigenvector is smaller for higher average energies. This result might indicate that a free particle (plane wave) moving with an energy E could be forced to lose all its energy when turning on a space-time periodic potential that oscillates with a frequency $\omega=E/\hbar$.

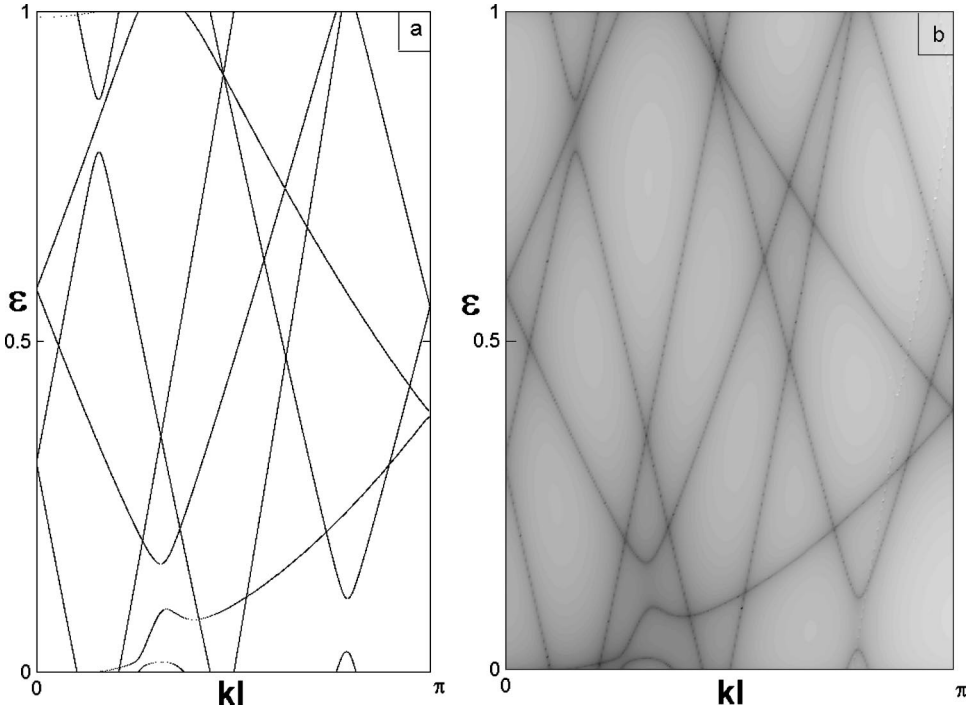

FIG. 6. $V_0=0, V_1=0.3, l=5$. (a) Quasienergy curves obtained by numerical diagonalization of the Floquet TM matrix. (b) Contour plot of the function $\Pi_8(\varepsilon, kl)$.

V. CONTRIBUTION OF THE NEGATIVE ENERGY CHANNELS

In this section we look at an interesting feature of the delta chain, which establishes a nice connection with the scattering properties of a single oscillating δ-function potential. In what follows, we assume the static potential is zero [$s_n=0$ in Eq. (38)] and ask the question: how do negative energy channels contribute to the Floquet eigenstates of the system? This question is motivated by the fact that, when the parameter l is large, numerical diagonalization of the TM matrix becomes very inaccurate because the terms $e^{ik_n l}$ become very large for negative energy channels (imaginary momentum k_n). Knowing how those channels contribute to the QE band structure is therefore an important question.

In Fig. 7(a) we show the location, in the QE band structure, of two eigenvectors of the system, and in Fig. 7(b) we

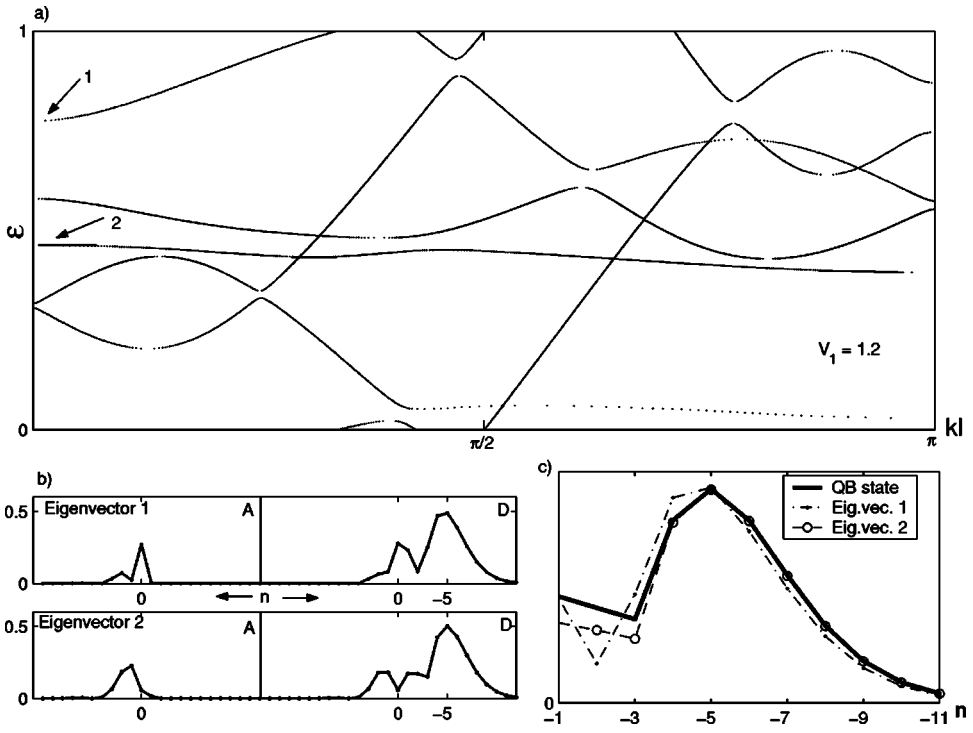

FIG. 7. (a) Quasienergy band structure for $V_0=0, V_1=1.2, l=5$. Arrows show locations, ($\varepsilon=0.775, k=0$) and ($\varepsilon=0.462, k=0$), of two eigenvectors plotted in (b). (b) Absolute value of the Floquet components of eigenvectors: (1) ($\varepsilon=0.775, k=0$); and (2) ($\varepsilon=0.462, k=0$). (c) Comparison of the negative energy contributions (D part) of the two eigenvectors in (b) with that of the quasibound state of a single δ-function potential.

plot the contribution to these eigenvectors from the various Floquet channels. It is important to notice the shape of D in the negative energy channels is very similar for the two eigenvectors despite their different quantum numbers (ε,k). Why is there a peak in channel -5 in all eigenvectors? What determines this structure? For a given amplitude of a_0, the structure of any eigenvector Ψ can be written in the following form:

$$\mathbf{\Psi}^T=(\mathbf{A}^T,\mathbf{D}^T), \tag{48}$$

where

$$\mathbf{A}^T=(\ldots,a_2,a_1,a_0,f^{\downarrow}_{-1}a_0,f^{\downarrow}_{-2}f^{\downarrow}_{-1}a_0,f^{\downarrow}_{-3}f^{\downarrow}_{-2}f^{\downarrow}_{-1}a_0,\ldots), \tag{49}$$

and

$$\mathbf{D}^T=(\ldots,\eta_2a_2,\eta_1a_1,\eta_0a_0,\eta_{-1}f^{\downarrow}_{-1}a_0,\eta_{-2}f^{\downarrow}_{-2}f^{\downarrow}_{-1}a_0,\ldots). \tag{50}$$

The structure of the negative energy part of the eigenvectors can be studied by looking at the sequence $[f^{\downarrow}_{-1},(f^{\downarrow}_{-2}f^{\downarrow}_{-1}),(f^{\downarrow}_{-3}f^{\downarrow}_{-2}f^{\downarrow}_{-1}),\ldots]$. Let us begin by defining the quantities ρ_n and b_n as

$$\rho_n\equiv\frac{1-e^{2ik_nl}}{e^{-ikl}-e^{ik_nl}},\quad b_n\equiv e^{ik_nl}-e^{ikl}, \tag{51}$$

so that

$$P_n=e^{-ik_nl}\rho_n,\quad R_n=e^{-ik_nl}b_n. \tag{52}$$

Using this in Eq. (43), we obtain an alternative expression for $f^{\downarrow}_{-n}$,

$$f^{\downarrow}_{-n}=\cfrac{ih_{-n}\rho_{-n+1}e^{-i(k_{-n+1}-k_{-n})l}}{b_{-n}+\cfrac{h^2_{-n-1}\rho_{-n-1}\rho_{-n}}{b_{-n-1}+\cfrac{h^2_{-n-2}\rho_{-n-2}\rho_{-n-1}}{b_{-n-2}+\cfrac{h^2_{-n-3}\rho_{-n-3}\rho_{-n-2}}{\vdots}}}}. \tag{53}$$

For $n>1$ this expression can be simplified. Since $\rho_{-n}\simeq e^{ikl}$ and $b_n\simeq -e^{ikl}$, $f^{\downarrow}_{-n}$ becomes

$$f^{\downarrow}_{-n}=\cfrac{ih_{-n}e^{-i(k_{-n+1}-k_{-n})l}}{1+\cfrac{h^2_{-n-1}}{1+\cfrac{h^2_{-n-2}}{1+\cfrac{h^2_{-n-3}}{\vdots}}}}. \tag{54}$$

From Eq. (54), one can conclude that for the negative energy channels, the positive momentum components, **A**, of the eigenvector decay exponentially with n; $f^{\downarrow}_{-n}\propto e^{-l/2n}$. This can be seen in Fig. 7(b) where it is evident that the negative energy components of **A** decay very quickly with n. In contrast, the vector, **D**, has a different structure, with a peak at $n=-5$. It is in this part of the eigenvector where the negative energy components contribute the most. If we had chosen to construct the TM matrix for translations to the left, then the A part would have shown the biggest contribution from the negative channels. From Eq. (33) and for negative energy channels $d_{-n}\simeq e^{-ik_{-n}l}a_{-n}$. Hence,

$$\frac{d_{-n}}{d_{-n+1}}=Z_{-n}\equiv\frac{ih_{-n}}{1+G_{-n}}, \tag{55}$$

where the CF, G_n, can be defined recursively as

$$G_n=\frac{h^2_{n-1}}{1+G_{n-1}}. \tag{56}$$

This function G_n is precisely the same function used to describe the transmission through a single oscillating δ function.[15] As shown in Appendix A, the ratio between the diagonal components, C_{-n}, of the transmission matrix for a single δ function is

$$\frac{C^*_{-n}}{C^*_{-n+1}}=-Z^{*2}_{-n},$$

where the (*) denotes evaluation at the pole of the S matrix.

The relationship actually goes further. In Appendix B we look at the quasibound state of the single δ-function potential and prove that its components (only the transmission part is considered, since the reflection should be identical for symmetry reasons) can be written as

$$\mathbf{V}^T_{QB}=(\ldots,1,Z^*_{-1},Z^*_{-1}Z^*_{-2},Z^*_{-1}Z^*_{-2}Z^*_{-3},\ldots) \tag{57}$$

whereas according to Eq. (55), the negative energy components of the vector, **D**, can be written as

$$\mathbf{D}^T=(\ldots,1,f^{\downarrow}_{-1},f^{\downarrow}_{-1}Z_{-2},f^{\downarrow}_{-1}Z_{-2}Z_{-3},\ldots). \tag{58}$$

The difference between Eqs. (58) and (59) is in the behavior of the function $f^{\downarrow}_{-1}(\varepsilon,k)$, which for a certain range of ε (because of its dependence on the Bloch momentum k) can be considerably different from $Z_{-1}(\varepsilon)$. The other difference concerns the fact that in Eq. (58) the Z_{-n} functions are evaluated at the pole whereas the functions in Eq. (59) are evaluated at different values along the bands. In Fig. 7(b) we show two eigenvectors of the infinite chain, and in Fig. 7(c) we compare the negative energy components of **D** with the

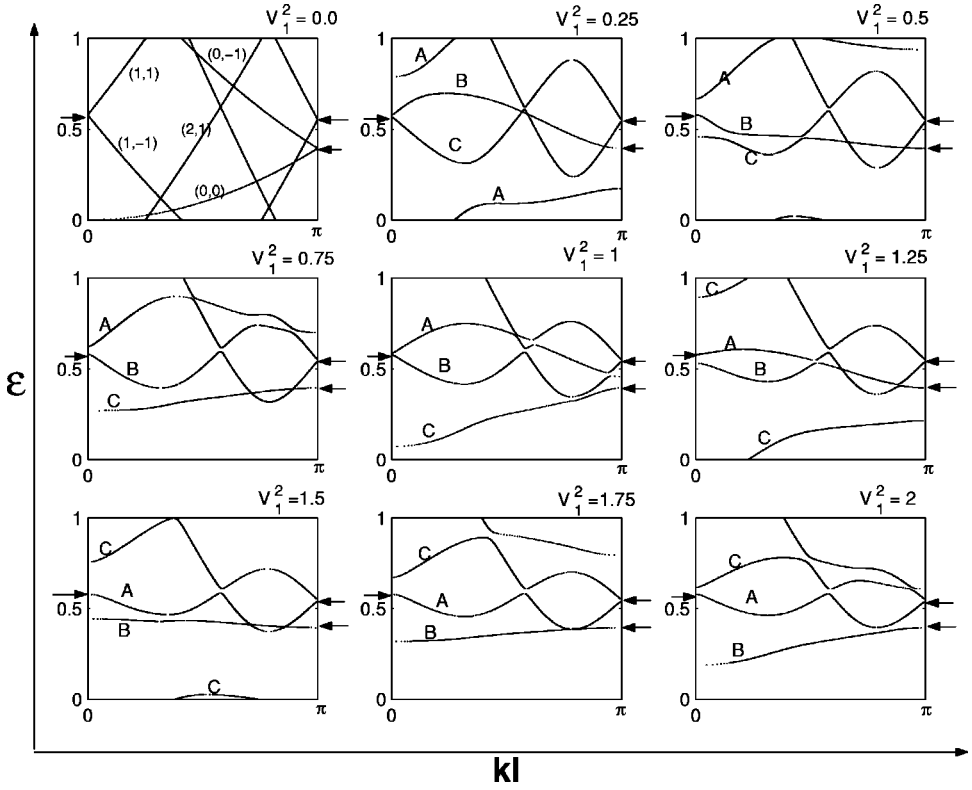

FIG. 8. Series of plots showing the evolution of QE bands (the four lowest in average energy) as the parameter V_1 is increased with fixed $V_0=0$ and $l=5$. Three of the bands (A,B,C) participate in a periodic exchange of identity. Band A initially related to unperturbed state (0,0), band B related to unperturbed states (1,1),(0,−1), and band C related to states (1,−1), (2,1). Arrows indicate the position of some of the fixed points in the QE band structure.

quasibound state of the single δ-function system. The agreement is quite good for all the eigenvectors that we considered. The reason for such agreement, which seems to be independent of the particular quasienergy of the eigenstate, is simple: the functions Z_{-n} are fairly smooth in the complex plane, therefore, their value at E^* and their value on the real axis are very close in most cases.

When the strength, V_1, is small, the different Floquet eigenstates are exponentially localized about the unperturbed states. As the strength V_1 increases and the eigenstates gain support in the negative energy channels, they develop a characteristic peak in those channels, which can actually dominate the structure of the vector, **D**, for the eigenstates with lowest average energy.

In general we can say that the structure of all FB eigenvectors of the infinite chain consists of two very distinct parts, the positive energy components which are sensitive to the Bloch-momentum k, and the negative energy components which are independent of k and are closely related to the quasibound state of the single δ-function potential. We expect this to be a general feature that should occur in other space-time periodic potentials such as an oscillating Kroenig-Penney potential.

VI. BAND DYNAMICS

In this section we discuss some general features of the behavior of the quasienergy bands as the strength V_1 of the oscillating potential is changed. In Sec. VI A we discuss the almost periodic behavior of the QE bands with lowest average energy as V_1 is changed. In Sec. VI B we discuss the existence of points in the QE band structure which are not affected by a change in the parameter V_1. Sec. VI C deals with the collapse (significant reduction of its width) of one of the QE bands for particular values of V_1.

A. Periodicity of the band structure

In the sequence of plots in Fig. 8, we show the bands associated with eigenvectors whose main support is on channels $n \leqslant 4$. We focus on these bands because they have especially interesting behavior as the parameter V_1 is changed. Inspection of these plots shows that as V_1 is varied, the band patterns come close to repeating their structure in an almost-periodic manner. In going from $V_1=0$ to $V_1=1.0$ there is one complete exchange of identity for each band: $(0,0) \rightarrow (0,-1)-(1,1)$, $(0,-1)-(1,1) \rightarrow (1,-1)-(2,1)$, $(1,-1)-(2,1) \rightarrow (0,0)$. From $V_1=1.0$ to $V_1=1.414$ there is another exchange. This periodicity occurs as a function of V_1^2. A similar quasiperiodic behavior was found for the transmission through a single oscillating delta-function potential,[15] where the dynamics of the zeros and poles of the system depend almost periodically on the parameter $a \equiv V_1^2$. The period in V_1^2 is one: the equivalent of panel $V_1^2=0.25$ is panel $V_1^2=1.25$, the equivalent of panel $V_1^2=0.5$ is $V_1^2=1.5$, and so on.

This periodicity is another manifestation of the correlation between the structure of the quasibound state in the single delta scattering problem and the structure of the eigenvectors with support in the lowest energy channels in the infinite chain.

B. Fixed points in the band structure

Suppose that before we turn on the oscillating potential, we have a state which is a superposition of two plain waves,

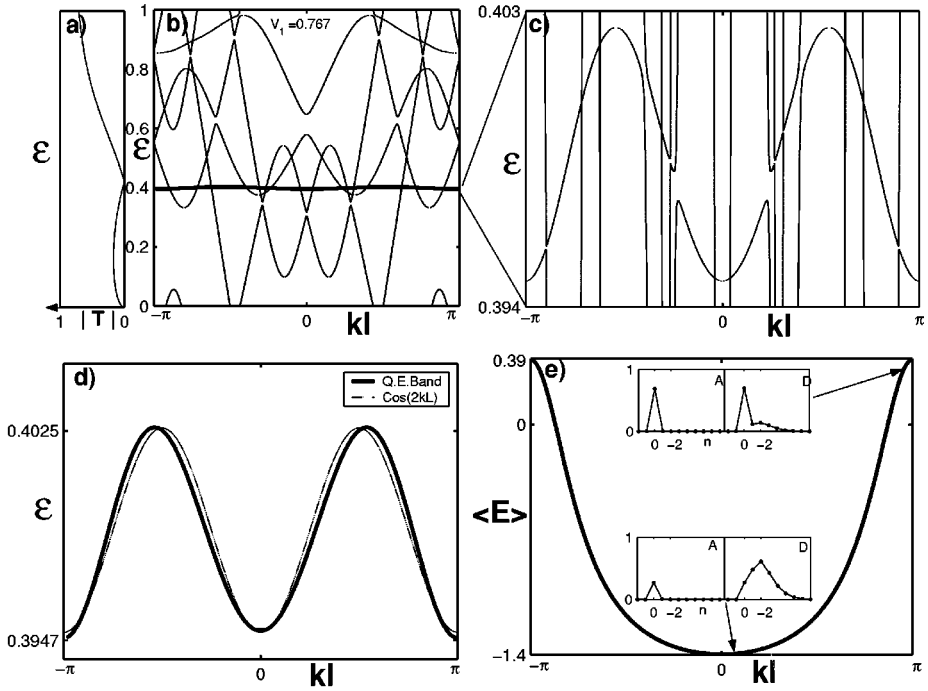

FIG. 9. (a) The transmission probability for a single oscillating δ-function potential as a function of quasienergy for $V_0=0, V_1=0.767, l=5$. (b) The quasienergy band structure of the infinite chain for $V_0=0, V_1=0.767, l=5$. The collapsed QE band is the thick line. (c) Magnification of the region in (b) occupied by the collapsed band. (d) The band (solid line) without the small avoided crossings with higher energy bands (diabatic representation). The function $\cos(2kl)$ is plotted for comparison (dot-dashed line). (e) The average energy along the collapsed band and the components of eigenstates from two different locations on the collapsed band.

in particular $\phi_n(x)=(1/2i)(e^{ik_nx}-e^{-ik_nx})=\sin(k_nx)$. If k_n satisfies the condition, $k_n=m\pi/l$ with $-\infty\leqslant m\leqslant\infty$, then $\sin(k_nl)=0$, which means that the wave function has nodes at the location of the δ functions. This implies that this particular state will not be affected as the potential is turned on (whether the δ-function potential is oscillating or not). This state is a Bloch state since it is periodic in space and it must belong to a band of the perturbed system. Therefore, for an infinite chain of δ functions, oscillating or not, there are fixed points in the band structure, in the sense that for any V_1 and V_0 there is always a band attached to the points that satisfy the condition $k_n=m\pi/l$. This is a special feature of the delta function potential. The fixed points are at the edges (m odd) and the center (m even) of the Brillouin zone. For $l=5$, we can obtain the location in quasienergy of the fixed points,

$$\sqrt{\varepsilon_{m,n}+n}=m\pi/l. \tag{59}$$

From this and the additional condition $0\leqslant\varepsilon_{m,n}\leqslant 1$ we obtain the first three, $\varepsilon_{0,1}=0.395$, $\varepsilon_{1,2}=0.579$, and $\varepsilon_{3,3}=0.553$. The value $\varepsilon_{0,0}=0$ is not important because the wave function of this state vanishes everywhere.

These three fixed points have been marked with arrows in the different panels in Fig. 8. It is important to mention that there are an infinite number of these points. In the panels in Fig. 8, only those associated with the positive energy channels, $n\leqslant 4$, are shown. The higher energy channels are not coupled in a significant way with the bands shown and do not produce any significant change in them.

C. Band collapse

As can be seen in Fig. 9, near the value $V_1=0.767$, one of the three QE bands that participated in the exchange described in Sec. VI A becomes practically flat, that is, the width of that QE band has collapsed to its minimum value. This collapse occurs almost periodically as a function of V_1^2. Collapse of QE bands in a periodic potential driven by an oscillating electric field has been studied before using one-band and two-band approximations.[2] It was shown there that in the single-band nearest-neighbor tight binding approximation, the collapse is complete (the width of the band goes to zero) and is determined by the zeros of the Bessel function J_0. In the same paper, numerical calculations show that the collapse is not complete as it is expected from the von Neumann-Wigner non-crossing rule.[16]

The probability current associated with an eigenstate in a collapsed band is very small. For $l=5$, only the positive energy components of an eigenstate could contribute to this current since the current due to the negative energy components is already very small (it decays exponentially with l). Because of this, each oscillating δ function in the chain must reflect the incident positive energy components of an eigenstate in a collapsed band. This is only possible if the location in quasienergy of the collapsed band is close to the quasienergy value for which a transmission zero occurs in a single δ-function potential.[15]

In Fig. 9(a), the transmission probability through one δ function has been plotted alongside the band structure of the infinite chain shown in Fig. 9(b). These figures show that the location of the collapsed band and the location of the zero of transmission are very close. Other collapses are expected for values of V_1 that satisfy the approximate relation $V_1^2\ (\mathrm{mod}1)\approx 0.767$. A relationship between the suppression of tunneling and band collapse has been pointed out before by Gomez-Llorente *et al.*,[17] although within the two-band approximation.

In Fig. 9(c), we enlarge the region occupied by the collapsed band. It reveals that the band has a finite width $\Delta \approx 0.008\hbar\omega$. Several avoided crossings with other bands can be seen. In Fig. 9(c) we only needed to include Floquet channels with $n \leqslant 1$ in the calculation , which shows that the basic structure of the band is determined by the coupling between the first propagating channel $(n=0)$ and the negative energy channels. Another way to obtain this basic structure is by using the diabatic representation,[18,19] where all avoided crossings with a gap smaller than a certain value are replaced by crossings. In Fig. 9(d), superimposed on the band is a plot of the function $\cos(2kl)$, which corresponds to the shape of the band if only nearest-neighbor interaction is allowed. The relative displacement of the maxima in the two curves indicates that there is a small amount of direct coupling between non-adjacent cells. In Fig. 9(c) we show the average energy of the eigenstate associated with the collapsed band and also the structure of two eigenstates at the points indicated. Near the edges of the Brillouin zone (the fixed point) the structure of the eigenstate is dominated by the structure of the unperturbed state, $\sin(k_0 x)$, which carries no current. The energy of the Floquet eigenstate near these points is therefore positive. As one moves from the edge to the center of the Brillouin zone the negative energy channels dominate and the average energy becomes negative.

It has been shown before that a relationship exists between dynamical suppression of tunneling and band collapse. In this work we have shown a relationship between dynamical suppression of transmission and band collapse. Other localized potentials such as the square well (or barrier) have been shown to have transmission zeros (resonances)[20,21] and therefore one might expect to observe QE band collapses associated with periodic chains of these potentials.

VII. CONCLUSIONS

We studied the dynamical properties of a spatially periodic chain of oscillating delta-function potentials, using two basic methods: degenerate perturbation theory and the Floquet translation matrix. Degenerate perturbation theory was developed to give a physical picture for the avoided crossings in the perturbative regime. The translation matrix method was developed as a more efficient method to calculate the eigenstates of the system. Also we were able to show an important relation with the scattering of a single δ-function potential.

Analysis of the average energy of the eigenstates of the system when a harmonic (frequency ω) perturbation is present reveals an interesting effect when the energy of the unperturbed system is close to a multiple of $\hbar\omega$. Turning on the harmonic space-periodic potential might cause the particle to give away all its energy (emit photons). This might provide a means of ''cooling'' atoms in a standing light-wave field.

We find that the lowest (in average energy) bands of the infinite chain can be considered the ''quasibound state bands'' in the following sense: their average energy is mostly negative (the corresponding eigenstates have their main support in the negative energy channels) and their structure is very similar to the structure of the quasibound state of a single δ-function potential. In Appendix B we provided a simple procedure to calculate the components of a quasibound state associated with one of the poles of an S matrix.

We studied the dynamics of the band structure as a function of the strength of a time periodic potential and found that the lowest (in average energy) bands are strongly affected by this parameter and show an almost periodic dependance on it, with successive exchanges of identity between them.

We identified points in the quasienergy band structure related with standing waves whose nodes correspond to the location of the oscillating δ functions in the chain. At these points (at the edge and center of the momentum Brillouin zone) one of the bands that participate in an avoided crossing remains pinned as the strength of the oscillating potential is changed.

We found that for certain values of the strength of the oscillating potential, the width of one of the QE bands becomes very small. This phenomenon has been called in the literature ''band collapse.'' It provides a possible mechanism to produce highly non-dispersive (coherent) states in a waveguide or superlattice. We found that the ''collapse'' is related to the dynamical quenching of the transmission through a single oscillating δ-function potential.

ACKNOWLEDGMENTS

Authors D.F.M. and L.E.R. wish to thank the Welch Foundation, Grant No. F-1051, NSF Grant No. INT-9602971, and DOE Contract No. DE-FG03-94ER14405 for partial support of this work. Author G.A.L.A. acknowledges partial support from CONACIT Project No. 26163-E.

APPENDIX A

For a single oscillating delta-function potential, it has been shown[15] that the elastic transmission amplitude C_n obeys an equation of the form

$$C_n = \frac{1}{F_n + G_n} \tag{A1}$$

with

$$F_n(\epsilon) = 1 + \frac{h_n^2(\epsilon)}{F_{n+1}(\epsilon)}, \tag{A2}$$

and

$$G_n(\epsilon) = \frac{h_{n-1}^2(\epsilon)}{1 + G_{n-1}(\epsilon)}. \tag{A3}$$

Therefore,

$$\frac{C_{-n}}{C_{-n+1}} = \frac{F_{-n+1}}{1 + G_{-n}}. \tag{A4}$$

When this expression is evaluated at the value of the quasienergy for which the S matrix has poles on each channel, we obtain (* indicates that the corresponding function is evaluated at the pole) $F^*_{-n+1} = -G^*_{-n+1}$, and therefore,

$$\frac{C^*_{-n}}{C^*_{-n+1}} = \frac{F^*_{-n+1}}{1 + G^*_{-n}} = -\frac{G^*_{-n+1}}{1 + G^*_{-n}} = -\frac{h^{2*}_{-n}}{(1 + G^*_{-n})^2} = -Z^{*2}_{-n}. \tag{A5}$$

APPENDIX B

A quasibound state associated with the pole of an S matrix can be found using the following argument. In general, any complex symmetric matrix, for example the S matrix in the complex plane, with n distinct eigenvalues can be written in the form[23]

$$\mathbf{S}=\mathbf{V}D\mathbf{V}^T, \tag{B1}$$

where D is a diagonal matrix. This can be written as

$$\mathbf{S}=\alpha_1\mathbf{V}_1\wedge\mathbf{V}_1^T+\alpha_2\mathbf{V}_2\wedge\mathbf{V}_2^T+\ \ldots, \tag{B2}$$

where $\alpha_1,\alpha_2,\ldots$ are the diagonal elements of $\mathbf{D}$ (which are proportional to the eigenvalues of S) and $\mathbf{V}_1,\mathbf{V}_2,\ldots$ are the columns of $\mathbf{V}$. As we approach a pole of the S matrix, $E\rightarrow E^*$, and one of the eigenvalues of $\mathbf{S}$ diverges. Therefore, $S\rightarrow S^*$, where

$$S^*=\alpha\mathbf{V}_{\mathrm{QB}}\wedge\mathbf{V}_{\mathrm{QB}}^T,$$

with

$$\alpha\rightarrow\infty \quad \text{as} \quad E\rightarrow E^*. \tag{B3}$$

$\mathbf{V}_{\mathrm{QB}}$ is the quasibound state, and it does not correspond to a square integrable wave-function. We define it as the eigenvector of S whose eigenvalue diverges at the pole. Now we proceed to show, using the exact solution for the S matrix of the single δ-function potential that, at the pole location, $\mathbf{S}$ can be written in this way and we will find the corresponding components of $\mathbf{V}_{\mathrm{QB}}$.

The diagonal elements of the transmission matrix are given by the quantities C_n. From this diagonal one can produce the rest of this matrix by using the functions f_n as defined in Ref. 15. The S matrix (near the pole) can be written as (only the transmission components are shown)

$$\mathbf{S}^*=\begin{pmatrix} \ddots & \vdots & \vdots & \vdots & \vdots & \\ \cdots & 1 & 1/Z_{-1}^* & 1/(Z_{-1}^*Z_{-2}^*) & 1/(Z_{-1}^*Z_{-2}^*Z_{-3}^*) & \cdots \\ \cdots & Z_{-1}^* & 1 & 1/Z_{-2}^* & 1/(Z_{-3}^*Z_{-2}^*) & \cdots \\ \cdots & Z_{-1}^*Z_{-2}^* & Z_{-2}^* & 1 & 1/Z_{-3}^* & \cdots \\ \cdots & Z_{-1}^*Z_{-2}^*Z_{-3}^* & Z_{-2}^*Z_{-3}^* & Z_{-3}^* & 1 & \cdots \\ & \vdots & \vdots & \vdots & \vdots & \ddots \end{pmatrix} D, \tag{B4}$$

with D a diagonal matrix with diagonal elements $D=(\ldots C_0^*,C_{-1}^*,C_{-2}^*\ldots)$. In the above expression we made use of the fact that to go down on a column starting from the diagonal matrix multiplies by Z_n^*, and to go up on a column from the diagonal matrix element divides by Z_n^* (this is only true at the pole, where $F_n^*=-G_n^*$). From this, and using $D=C_0^*(\ldots 1,Z_{-1}^{*2},Z_{-1}^{*2}Z_{-2}^{*2},Z_{-1}^{*2}Z_{-2}^{*2}Z_{-3}^{*2}\ldots)$, we write $\mathbf{S}^*$ as

$$\mathbf{S}^*=C_0^*\begin{pmatrix} \ddots & \vdots & \vdots & \vdots & \\ \cdots & 1 & Z_{-1}^* & Z_{-1}^*Z_{-2}^* & \cdots \\ \cdots & (Z_{-1}^*) & Z_{-1}^*(Z_{-1}^*) & Z_{-1}^*Z_{-2}^*(Z_{-1}^*) & \cdots \\ \cdots & (Z_{-1}^*Z_{-2}^*) & Z_{-1}^*(Z_{-1}^*Z_{-2}^*) & Z_{-1}^*Z_{-2}^*(Z_{-1}^*Z_{-2}^*) & \cdots \\ \cdots & (Z_{-1}^*Z_{-2}^*Z_{-3}^*) & Z_{-1}^*(Z_{-1}^*Z_{-2}^*Z_{-3}^*) & Z_{-1}^*Z_{-2}^*(Z_{-1}^*Z_{-2}^*Z_{-3}^*) & \cdots \\ & \vdots & \vdots & \vdots & \ddots \end{pmatrix}. \tag{B5}$$

This expression has exactly the form anticipated in the discussion about the form of the S matrix near the pole, since it can be written as an external product,

$$\mathbf{S}^*=C_0^*\mathbf{V}_{\mathrm{QB}}\wedge\mathbf{V}_{\mathrm{QB}}^T, \tag{B6}$$

with

$$\mathbf{V}_{\mathrm{QB}}^T=(\ldots,1,Z_{-1}^*,Z_{-1}^*Z_{-2}^*,Z_{-1}^*Z_{-2}^*Z_{-3}^*,\ldots), \tag{B7}$$

and C_0^* diverging at the pole.

[1] For a good review, see E.E. Mendez and Gerald Bastard, Phys. Today **46** (6), 34 (1993).
[2] M. Holthaus, Phys. Rev. Lett. **69**, 351 (1992); M. Holthaus and D.W. Hone, Phys. Rev. B **47**, 6499 (1993); M. Holthaus and D.W. Hone, *ibid.* **49**, 16 605 (1994); K. Drese and M. Holthaus, J. Phys.: Condens. Matter **8**, 1193 (1996).
[3] D.H. Dunlap and V.M. Kenkre, Phys. Rev. B **34**, 3625 (1986); Phys. Lett. A **127**, 438 (1988); S. Raghavan, V.M. Kenkre, D.H. Dunlap, A.R. Bishop, and M.I. Salkola, Phys. Rev. A **54**, R1781 (1996).
[4] B.J. Keay, S.J. Allen, Jr., J. Galan, J.P. Kaminsky, K.L. Campman, A.C. Gossard, U. Bhattacharya, and M.J.W. Rodwell, Phys. Rev. Lett. **75**, 4098 (1995); B.J. Keay, S. Zeuner, S.J. Allen, Jr., K.D. Maranowski, A.C. Gossard, U. Bhattacharya, and M.J.W. Rodwell, Phys. Rev. Lett. **75**, 4102 (1995).
[5] H. Schanz, M.F. Otto, R. Ketzmerick, and T. Dittrich, Phys. Rev. Lett. **87**, 070601 (2001).
[6] I. Goychuk and P. Hänggi, in *Lecture Notes on Physics*, edited by J. Freund and T. Pöschel (Springer, Berlin, 2000), Vol. 557, pp. 7–20.
[7] R. Roncaglia, L. Bonci, F. M. Izrailev, B. J West, and P. Grigolini, Phys. Rev. Lett. **73**, 802 (1995).
[8] R. Utermann, T. Dittrich, and P. Hänggi, Phys. Rev. E **49**, 273 (1994).
[9] O. Bohigas, S. Tomsovic, and D. Ullmo, Phys. Rep. **223**, 43 (1993).
[10] D.A. Steck, W.H. Oskay, and M.G. Raizen, Science **293**, 274 (2001).
[11] W.K. Hensinger, H. Häffner, A. Browaeys, N.R. Heckenberg, K. Helmerson, C. McKenzie, G.J. Milburn, W.D. Phillips, S.L. Rolston, H. Rubinsztein-Dunlop, and B. Upcroft, Nature (London) **412**, 52 (2001).
[12] L. E. Reichl, in *The Transition to Chaos in Conservative Classical Systems: Quantum Manifestations* (Springer, New York, 1992).
[13] D.J. Thouless, Phys. Rev. B **27**, 6083 (1983).
[14] J.H. Hannay and R.J. McCraw, J. Phys. A **23**, 887 (1990).
[15] D.F. Martinez and L.E. Reichl, Phys. Rev. B **64**, 245315 (2001).
[16] J. von Neumann and E. Wigner, Phys. Z. **30**, 467 (1929), translated in R. S. Knox and A. Gold, *Symmetry in the Solid State* (Benjamin, New York 1964).
[17] E.M. Zanardy and J. M Gomez Llorente, Chem. Phys. **217**, 221 (1997).
[18] A.R. Kolovsky, S. Miyazaki, and R. Graham, Phys. Rev. E **49**, 70 (1994).
[19] T. Takami, Phys. Rev. Lett. **68**, 3371 (1992).
[20] W. Li and L.E. Reichl, Phys. Rev. B **60**, 15 732 (1999).
[21] M. Wagner, Phys. Rev. A **51**, 798 (1995).
[22] N. W. Ashcroft and N. D. Mermin, in *Solid State Physics* (Saunders College, Philadelphia, 1976).
[23] R. A. Horn and C. R. Johnson, in *Matrix Analysis* (Cambridge University Press, Cambridge, 1985).